Boundary Value Problems
a SpringerOpen Journal

RESEARCH Open Access

Effect of variable viscosity on vortex instability of non-Darcy free convection boundary layer flow adjacent to a non-isothermal horizontal surface in a porous medium

Ahmed M Elaiw[1,4*], Ahmed A Bakr[2,4] and Fuad S Ibrahim[3,5]

* Correspondence:
a_m_elaiw@yahoo.com
[1]Department of Mathematics, Faculty of Science, King Abdulaziz University, P.O. Box 80203, Jeddah 21589, Saudi Arabia
Full list of author information is available at the end of the article

Abstract

In this article, we study the effect of variable viscosity on the flow and vortex instability of non-Darcian free convection boundary layer flow on a horizontal surface in a saturated porous medium. The wall temperature is a power function of the distance from the origin. The variation of viscosity is expressed as an exponential function of temperature. The transformed boundary layer equations, which are developed using a non similar solution approach, are solved by means of a finite difference method. The analysis of the disturbance flow is based on linear stability theory. The local Nusselt number, critical Rayleigh number and the associated wave number at the onset of vortex instability are presented over a wide range of wall to ambient viscosity ratio parameters $\mu^* = \mu_w/\mu_\infty$. The variable viscosity effect is found to enhance the heat transfer rate and destabilize the flow for liquid heating, while the opposite trend is true for gas heating.

Keywords: vortex instability, porous media, variable viscosity, non-Darcy, free convection, finite difference method

1 Introduction

The problems of the vortex mode of instability in free and mixed convection flows over horizontal and inclined heated surfaces in saturated porous media have received considerable attention (see [1-11]). The instability mechanism is due to the presence of a buoyancy force component in the direction normal to the surface. The importance of the problems is due to a large number of technical applications, such as material transfer associated with the storage of radioactive nuclear waste, separation processes in the chemical industry, filtration, transpiration cooling, transport processes in aquifers, and ground water pollution. Some researchers considered Darcy model [1-5], others considered non-Darcy model [6-11]. A comprehensive literature survey on this subject can be found in the recent book by Nield and Bejan [12].

All of the studies mentioned previously dealt with constant viscosity. The fundamental analysis of convection through porous media with temperature dependent viscosity is driven by several contemporary engineering applications from the cooling of electronic devices to porous journal bearings and is important for studying the variations in

constitutive properties. The effect of variable viscosity for convective heat transfer through porous media has also been widely studied (e.g., [13-19]). The effect of variations in viscosity on the instability of flow and temperature fields are discussed by Kassoy and Zebib [13] and Gray et al. [14]. Lai and Kulacki [15] considered the variable viscosity effect for mixed convection along a vertical plate embedded in a saturated porous medium. The effect of variable viscosity on non-Darcy, free or mixed convection flow on a horizontal surface in a saturated porous medium is studied by Kumari [16]. Jayanthi and Kumari [17] studied the same problem presented in Kumari [16] for vertical surface. Afify [18] studied the effects of non-Darcy, variable viscosity and Hartmann-Darcy number on free convective heat transfer from an impermeable vertical plate embedded in a thermally stratified, fluid saturated porous medium for the case of power-law variation in the wall temperature. In [15-18], the viscosity of the fluid is assumed to vary as an inverse linear function of temperature, whereas in [19], the variation of viscosity with temperature is represented by an exponential function.

The effects of variable viscosity on the vortex instability of horizontal free and mixed convection boundary layer flows in a saturated porous medium for isothermal and non-isothermal surfaces are studied by Jang and Leu [19] and Elaiw et al. [20], respectively. However, the effect of variable viscosity on the flow and vortex instability of non-Darcian free convection boundary layer flow over a non-isothermal horizontal plate does not seem to have been investigated. This motivated the present investigation.

The purpose of this article is to examine in details the effect of temperature-dependent viscosity on the flow and vortex instability of a horizontal non-Darcian free convection boundary layer flow in a saturated porous medium with variable wall temperature. This is accomplished by considering the Ergun model equation of motion. The variation of viscosity with temperature is represented by an exponential function, which is more accurate than linear function especially for large temperature differences. The transformed boundary layer equations, which are given using a non similar solution approach, are solved by means of a finite difference method. The stability analysis is based on the linear stability theory. The resulting eigenvalue problem is solved using a finite difference scheme.

2 Analysis

2.1 The main flow

We consider a semi-infinite non-isothermal horizontal surface (T_w) embedded in a porous medium (T_∞) as shown in Figure 1, where x represents the distance along the plate from its leading edge, and y the distance normal to the surface. The wall temperature is assumed to be a power function of x, i.e., $T_w(x) = T_\infty + Ax^\lambda$, where A is a constant and λ is the parameter representing the variation of the wall temperature. In order to study transport through high porosity media, the original Darcy model is improved by including inertia. For the mathematical analysis of the problem we assume that, (i) local thermal equilibrium exists between the fluid and the solid phase, (ii) the physical properties are constant, except for the viscosity μ and the density ρ in the bouncy force, (iii) Ergun non-Darcy model [21] is considered, and (iv) the Boussinesq approximation is valid. With these assumptions, the governing equations are given by:

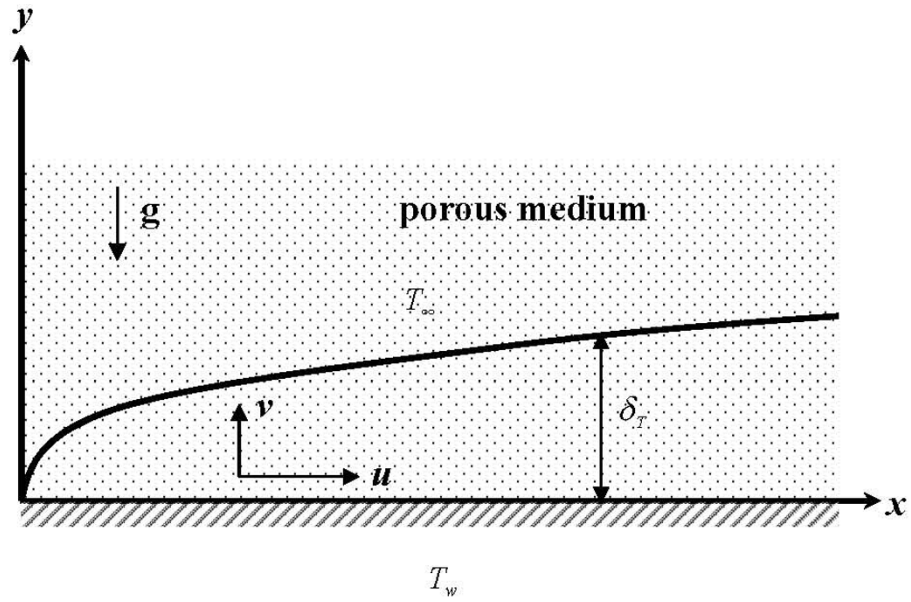

Figure 1 The physical model and coordinate system.

$$\frac{\partial u}{\partial x} + \frac{\partial v}{\partial y} = 0, \tag{1}$$

$$u + \frac{K^*}{v}u^2 = -\frac{K}{\mu}\frac{\partial P}{\partial x}, \tag{2}$$

$$v + \frac{K^*}{v}v^2 = -\frac{K}{\mu}\left(\frac{\partial P}{\partial y} + \rho g\right), \tag{3}$$

$$u\frac{\partial T}{\partial x} + v\frac{\partial T}{\partial y} = \alpha\frac{\partial^2 T}{\partial y^2}, \tag{4}$$

where $\rho = \rho_\infty[1 - \beta(T - T_\infty)]$ is the fluid density. Note that the second term on the left-hand side of Equations (2) and (3) represents the inertia force, where K^* is the inertia coefficient in Ergun model. As $K^* = 0$, Equations (2) and (3) reduce to Darcy model.

The viscosity of the fluid μ is assumed to vary with temperature according to the following exponential form

$$\mu = \mu_\infty e^{A_1\left(\frac{T-T_\infty}{T_w-T_\infty}\right)}, \tag{5}$$

where μ_∞ is the absolute viscosity at ambient temperature and A_1 is a constant adopted from the least square fitting for a particular fluid. Formula (5) is a generalization of that used in [19], where the wall temperature is taken to be constant.

The pressure terms appearing in Equations (2) and (3) can be eliminated through cross-differentiation. The boundary layer assumption yields $\partial/\partial x \ll \partial/\partial y$ and $v \ll u$. With ψ being a stream function such that $u = \partial\psi/\partial y$ and $v = -\partial\psi/\partial x$, the Equations (1)-(4) become

$$\left(\mu + 2\rho_\infty K^* \frac{\partial \psi}{\partial \gamma}\right) \frac{\partial^2 \psi}{\partial \gamma^2} + u \frac{\partial \mu}{\partial \gamma} = -K\rho_\infty g\beta \frac{\partial T}{\partial x}, \tag{6}$$

$$\frac{\partial \psi}{\partial \gamma} \frac{\partial T}{\partial x} - \frac{\partial \psi}{\partial x} \frac{\partial T}{\partial \gamma} = \alpha \frac{\partial^2 T}{\partial \gamma^2}. \tag{7}$$

The boundary conditions are defined as follows

$$\begin{aligned} &v(x,0) = -\frac{\partial \psi}{\partial x} = 0,\ T(x,0) = T_w = T_\infty + Ax^\lambda, \\ &u(x,\infty) = 0, \qquad\quad T(x,\infty) = T_\infty. \end{aligned} \tag{8}$$

By introducing the following similarity variables:

$$\begin{aligned} &\eta(x,\gamma) = \frac{\gamma}{x} Ra_x^{1/3}, \quad f(\xi,\eta) = \frac{\psi(x,\gamma)}{\alpha Ra_x^{1/3}}, \\ &\theta(\xi,\eta) = \frac{T - T_\infty}{T_w - T_\infty},\ \xi = \left(\frac{x}{d}\right)^{(2\lambda-1)/3}, \end{aligned} \tag{9}$$

Equations (5)-(7) become

$$\frac{\mu}{\mu_\infty} = e^{A_1\left(\frac{T-T_\infty}{T_w-T_\infty}\right)} = (\mu^*)^\theta, \tag{10}$$

$$(1 + 2ErRa_d^{2/3}\xi(\mu^*)^{-\theta} f\prime) f\prime\prime = -(\ln \mu^*) f\prime\theta\prime - (\mu^*)^{-\theta}\left(\lambda\theta + \frac{\lambda-2}{3}\eta\theta\prime + \frac{2\lambda-1}{3}\xi\frac{\partial\theta}{\partial\xi}\right), \tag{11}$$

$$\theta\prime\prime = \left(\lambda\theta + \frac{2\lambda-1}{3}\xi\frac{\partial\theta}{\partial\xi}\right) f\prime - \left(\frac{\lambda+1}{3} f + \frac{2\lambda-1}{3}\xi\frac{\partial f}{\partial\xi}\right)\theta\prime, \tag{12}$$

where $\mu^* = \mu_w/\mu_\infty = e^{A_1}$is the wall to ambient viscosity ratio parameter, $Ra_x = \frac{\rho_\infty g\beta K(T_w - T_\infty)x}{\alpha\mu_\infty}$ is the local Rayleigh number, $Ra_d = \frac{\rho_\infty g\beta K A d^{\lambda+1}}{\alpha\mu_\infty}$ is the Rayleigh number based on the pore diameter and $Er = \frac{K^*\alpha}{d\nu_\infty}$ is the Ergun number.

The boundary conditions are transformed as follows:

$$\begin{aligned} &f(\xi,0) = 0, \quad \theta(\xi,0) = 1, \\ &f\prime(\xi,\infty) = 0,\ \theta(\xi,\infty) = 0, \end{aligned} \tag{13}$$

where the primes denote the derivatives with respect to η. The velocity components and the heat transfer coefficient in term of the local Nusselt number are given by:

$$u(x,\gamma) = \frac{\alpha Ra_x^{2/3}}{x} f\prime(\xi,\eta), \tag{14}$$

$$v(x,\gamma) = -\frac{\alpha Ra_x^{1/3}}{3x}\left((\lambda+1) f(\xi,\eta) + (\lambda-2)\,\eta f\prime(\xi,\eta) + (2\lambda-1)\,\xi\frac{\partial f(\xi,\eta)}{\partial\xi}\right), \tag{15}$$

$$Nu_x \Big/ Ra_x^{1/3} = -\theta\prime(\xi,0). \tag{16}$$

2.2 The disturbance flow

The standard linear stability method yields the following:

$$\frac{\partial u_1}{\partial x} + \frac{\partial v_1}{\partial y} + \frac{\partial w_1}{\partial z} = 0, \tag{17}$$

$$\mu_0 u_1 + \mu_1 u_0 + 2K^* \rho_\infty u_0 u_1 = -K \frac{\partial P_1}{\partial x}, \tag{18}$$

$$\mu_0 v_1 + \mu_1 v_0 + 2K^* \rho_\infty v_0 v_1 = -K \left(\frac{\partial P_1}{\partial y} - \rho_\infty g \beta T_1 \right), \tag{19}$$

$$\mu_0 w_1 = -K \frac{\partial P_1}{\partial z}, \tag{20}$$

$$u_0 \frac{\partial T_1}{\partial x} + v_0 \frac{\partial T_1}{\partial y} + u_1 \frac{\partial T_0}{\partial x} + v_1 \frac{\partial T_0}{\partial y} = \alpha \left[\frac{\partial^2 T_1}{\partial x^2} + \frac{\partial^2 T_1}{\partial y^2} + \frac{\partial^2 T_1}{\partial z^2} \right]. \tag{21}$$

where the subscripts 0 and 1 signify the mean flow and disturbance components, respectively.

Following the order of magnitude analysis method described in detail by Hsu et al. [1], the terms $\partial u_1/\partial x$ and $\partial^2 T_1/\partial x^2$ in Equations (17) and (21) can be neglected. The omission of $\partial u_1/\partial x$ in Equation (17) implies the existence of a disturbance stream function Ψ_1, such as

$$w_1 = \frac{\partial \Psi_1}{\partial y}, \quad v_1 = -\frac{\partial \Psi_1}{\partial z}. \tag{22}$$

Eliminating P_1 from Equations (18)-(20) with the aid of (22) leads to

$$u_0 \frac{\partial \mu_1}{\partial z} + (\mu_0 + 2K^* \rho_\infty u_0) \frac{\partial u_1}{\partial z} = \mu_0 \frac{\partial^2 \Psi_1}{\partial x \partial y} + \frac{\partial \Psi_1}{\partial y} \frac{\partial \mu_0}{\partial x}, \tag{23}$$

$$-(\mu_0 + 2K^* \rho_\infty v_0) \frac{\partial^2 \Psi_1}{\partial z^2} + v_0 \frac{\partial \mu_1}{\partial z} = \mu_0 \frac{\partial^2 \Psi_1}{\partial y^2} + \frac{\partial \mu_0}{\partial y} \frac{\partial \Psi_1}{\partial y} + K \rho_\infty g \beta \frac{\partial T_1}{\partial z}, \tag{24}$$

$$u_0 \frac{\partial T_1}{\partial x} + v_0 \frac{\partial T_1}{\partial y} + u_1 \frac{\partial T_0}{\partial x} - \frac{\partial \Psi_1}{\partial z} \frac{\partial T_0}{\partial y} = \alpha \left(\frac{\partial^2 T_1}{\partial y^2} + \frac{\partial^2 T_1}{\partial z^2} \right). \tag{25}$$

As in Hsu et al. [1], we assume that the three-dimensionless disturbances for neutral stability are of the form

$$(\Psi_1, u_1, T_1) = \left[\overline{\Psi}(x, y), \bar{u}(x, y), \bar{T}(x, y) \right] e^{iaz}, \tag{26}$$

where a is the spanwise periodic wave number. Substituting Equation (26) into Equations (23)-(25) yields

$$\bar{u} = \left(\frac{1}{1 + \frac{2K^*}{\nu_\infty} (\mu^*)^{-\theta} u_0} \right) \left[\frac{1}{ia} \left(\frac{\partial^2 \overline{\Psi}}{\partial x \partial y} + (\ln \mu^*) \frac{\partial \overline{\Psi}}{\partial y} \frac{\partial \theta}{\partial x} \right) - (\ln \mu^*) \frac{u_0 \bar{T}}{T_w - T_\infty} \right], \tag{27}$$

$$\frac{\partial^2\overline{\Psi}}{\partial\gamma^2}-a^2\left(1+\frac{2K^*}{\nu_\infty}(\mu^*)^{-\theta}v_0\right)\overline{\Psi}-iav_0(\ln\mu^*)\frac{\bar{T}}{T_w-T_\infty}+(\ln\mu^*)\frac{\partial\theta}{\partial\gamma}\frac{\partial\overline{\Psi}}{\partial\gamma}=-\frac{iaK\rho_\infty g\beta}{\mu_\infty}(\mu^*)^{-\theta}\bar{T}, \tag{28}$$

$$u_0\frac{\partial\bar{T}}{\partial x}+v_0\frac{\partial\bar{T}}{\partial\gamma}+\bar{u}\frac{\partial T_0}{\partial x}-ia\overline{\Psi}\frac{\partial T_0}{\partial\gamma}=\alpha\left(\frac{\partial^2\bar{T}}{\partial\gamma^2}-a^2\bar{T}\right). \tag{29}$$

Equations (27)-(29) are solved based on the local similarity approximation [22], wherein the disturbances are assumed to have weak dependence in the streamwise direction (i.e., $\partial/\partial x \ll \partial/\partial\eta$).

On applying the following transformations

$$k=\frac{ax}{Ra_x^{1/3}},\ F(\eta)=\frac{\overline{\Psi}}{i\alpha Ra_x^{1/3}},\ \Theta(\eta)=\frac{\bar{T}}{T_w-T_\infty}, \tag{30}$$

into Equations (27)-(29) leads to the following:

$$\begin{aligned}F''+(\ln\mu^*)\theta'F'-k^2\left(1-\frac{2ErRa_d^{2/3}}{Ra_x^{1/3}}\xi(\mu^*)^{-\theta}G_1\right)F\\ +\frac{k(\ln\mu^*)}{Ra_x^{1/3}}G_1\Theta=-kRa_x^{1/3}(\mu^*)^{-\theta}\Theta,\end{aligned} \tag{31}$$

$$\begin{aligned}\Theta''+G_3\Theta'-\left[k^2+\lambda f'-\frac{(\ln\mu^*)f'G_2}{1+2ErRa_d^{2/3}\xi(\mu^*)^{-\theta}f'}\right]\Theta\\ -\frac{G_2\left[\frac{\lambda-2}{3}\eta F''+\left(\frac{2\lambda-1}{3}+(\ln\mu^*)G_4\right)F'\right]}{kRa_x^{1/3}\left(1+2ErRa_d^{2/3}\xi(\mu^*)^{-\theta}f'\right)}=kRa_x^{1/3}\theta'F,\end{aligned} \tag{32}$$

with the boundary conditions

$$F(0)=F(\infty)=\Theta(0)=\Theta(\infty)=0, \tag{33}$$

where G_1 - G_4 are given by

$$\begin{aligned}G_1&=\frac{\lambda+1}{3}f+\frac{\lambda-2}{3}\eta f'+\frac{2\lambda-1}{3}\xi\frac{\partial f}{\partial\xi},\\ G_2&=\lambda\theta+\frac{\lambda-2}{3}\eta\theta'+\frac{2\lambda-1}{3}\xi\frac{\partial\theta}{\partial\xi},\\ G_3&=\frac{\lambda+1}{3}f+\frac{2\lambda-1}{3}\xi\frac{\partial f}{\partial\xi},\\ G_4&=\frac{\lambda-2}{3}\eta\theta'+\frac{2\lambda-1}{3}\xi\frac{\partial\theta}{\partial\xi},\end{aligned}$$

For fixed values of ξ, λ, k, Er, Ra_d, and μ^*, the solution F and Θ is an eigenfunction for the eigenvalue Ra_x. When $\mu^*=1$, $Er=Ra_d=\xi=0$, Equations (31) and (32) reduce to those presented in [1] and when $\mu^*=1$, $\xi=1$, $\frac{\partial}{\partial\xi}=0$, $\lambda=0.5$ they reduce to those given in [8]. It may also remarked that for $\lambda=Er=Ra_d=\xi=0$, Equations (31) and (32) reduce to those presented in Jang and Leu [19].

3 Numerical scheme

In this section, we compute the approximate values of Ra_x for Equations (31) and (32) with boundary conditions (33). An implicit finite difference method is used to solve first the base flow Equations (11) and (12) with boundary conditions (13). The results are stored for a fixed step size h, which is small enough to make an accurate linear interpolation between mesh point. The domain is $0 \le \eta \le \eta_\infty$, where η_∞ is the edge of the boundary layer of the basic flow. For a positive integer N, let $h = \eta_\infty/N$ and $\eta_i = ih$, $i = 0, 1, \ldots, N$. The problem is discretized with standard centered finite differences of order two, following Usmani [23]. The solution of the eigenvalue problem is achieved by using the subroutine GVLRG of the IMSL library, see [24].

4 Results and discussion

Numerical results for the local Nusselt number, neutral stability curves, critical Rayleigh numbers and associate wave numbers at the onset of vortex instability for wall to ambient viscosity ratio parameter μ^* ranging from 0.1 to 10 and Ergun number Er ranging from 0.1 to 0.6 are presented. The effect of the non uniform temperature profile

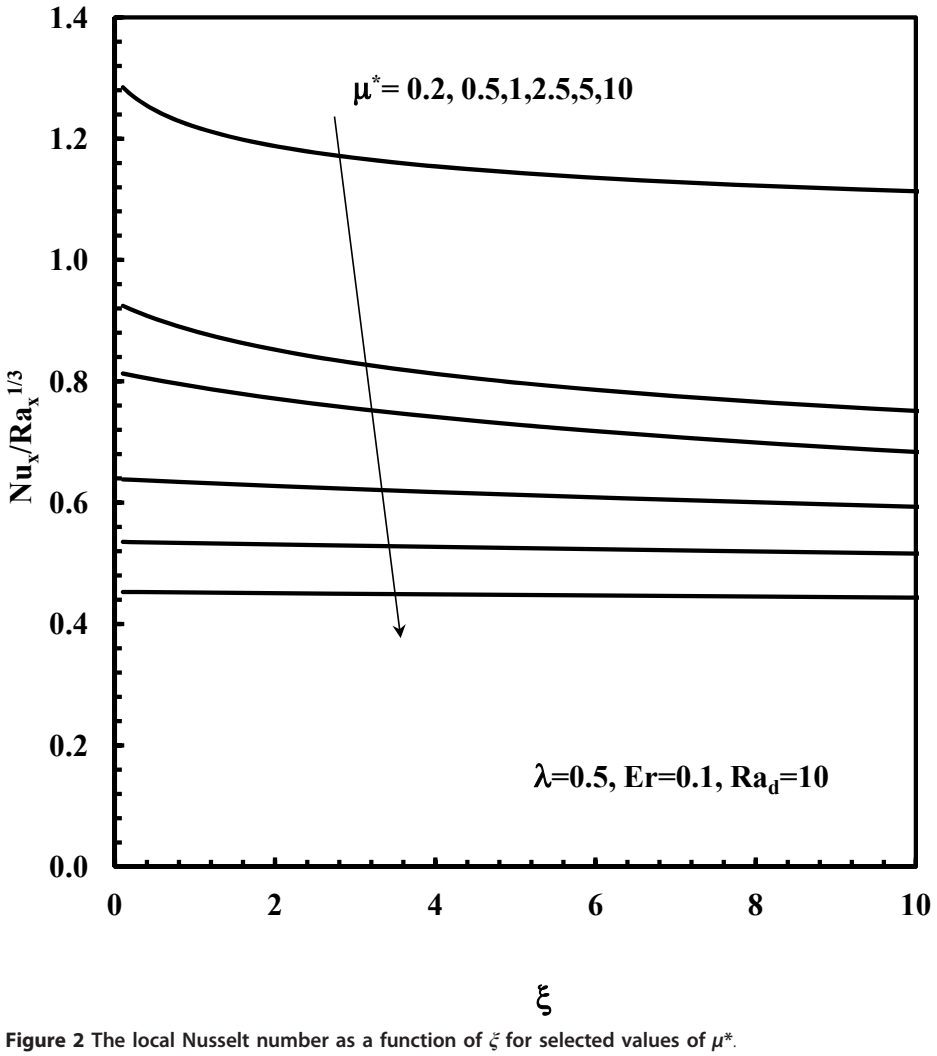

Figure 2 The local Nusselt number as a function of ξ for selected values of μ^*.

on the wall is also studied, and corresponds to variation of the parameter λ from 0.5 to 2. It is known that as the temperature is increased, the gas viscosity increases and the liquid viscosity decreases [19]. Therefore, for a heated wall, values of $\mu^* > 1$ corresponds to the case of gas heating, values of $\mu^* < 1$ corresponds to the case of liquid heating.

The local Nusselt number as a function ξ for various values of μ^*, Er, and λ is shown in Figures 2 and 3. The heat transfer rate is observed to be more than the constant-viscosity case for liquids $\mu^* < 1$ and it has the opposite trend for gases $\mu^* > 1$. Further, a lower local Nusselt number is seen to occur with greater values of Er and ξ. Furthermore, a higher Nusselt number is seen to occur with greater values of λ.

Figures 4 and 5, respectively, show the neutral stability curves, in terms of Rayleigh numbers Ra_x and the dimensionless wave number k for selected values of μ^* and ξ.

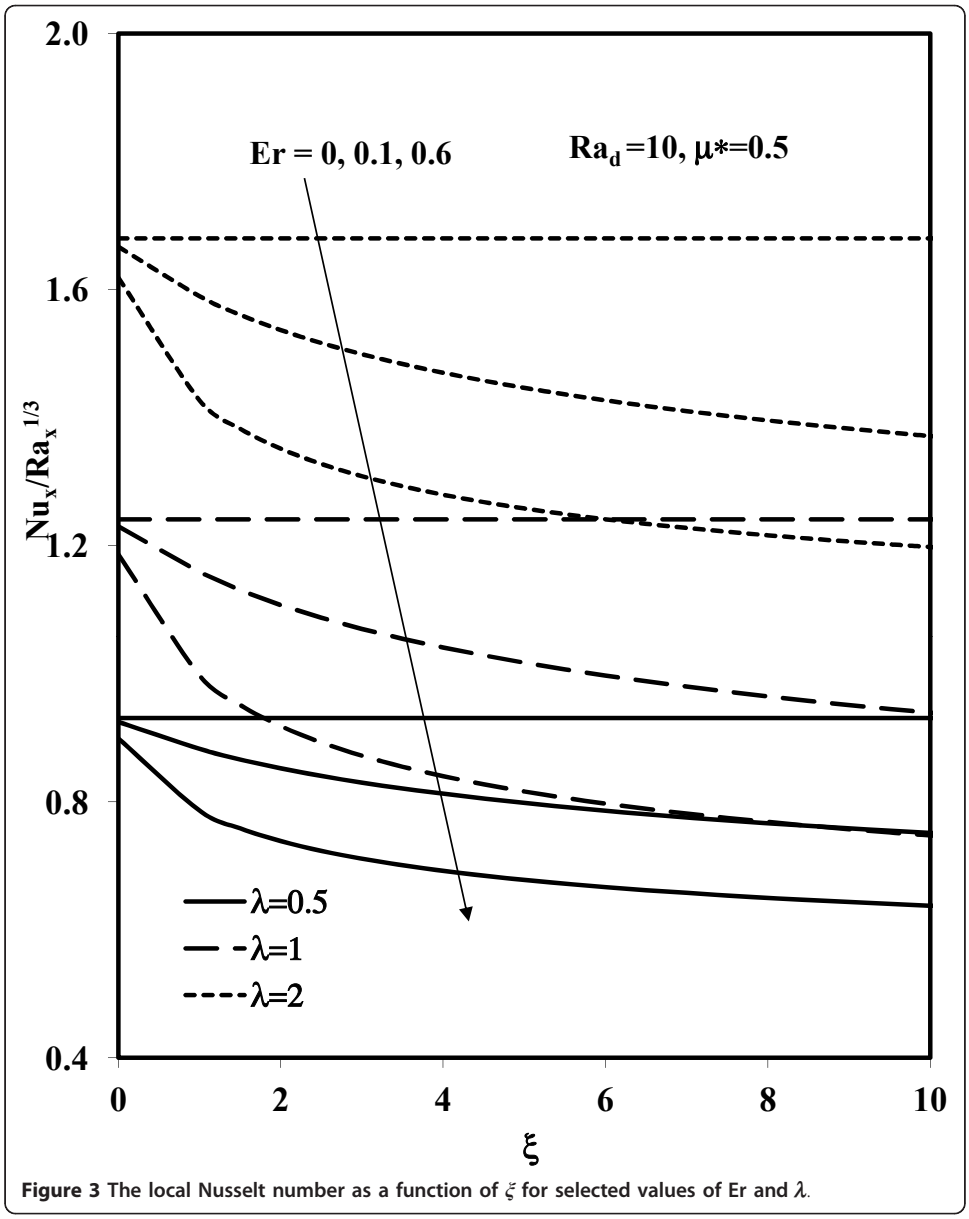

Figure 3 The local Nusselt number as a function of ξ for selected values of Er and λ.

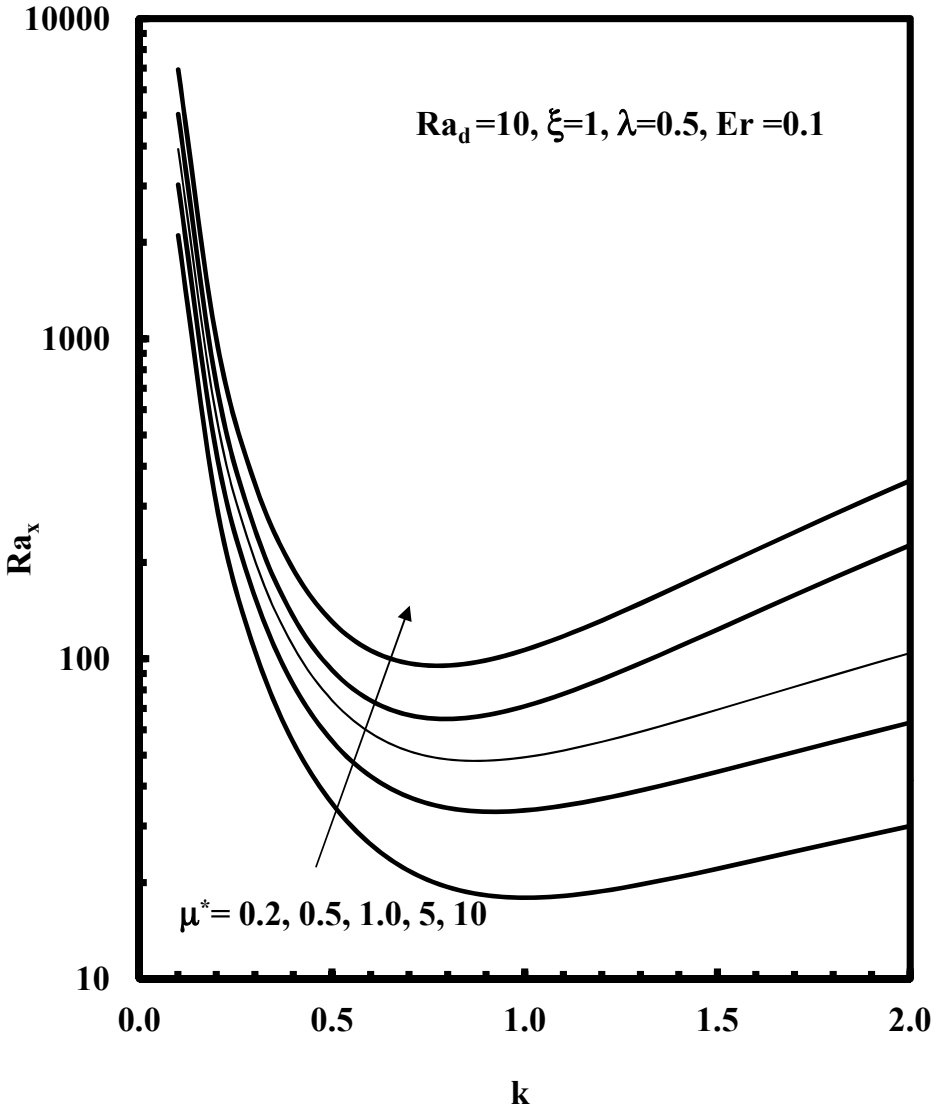

Figure 4 Neutral stability curves for selected values of μ^*.

Observe that as μ^* and ξ increase, the neutral stability curves shift to a higher Rayleigh number Ra_x. On the other hand, for liquid heating $\mu^* < 1$, the neutral stability curves shift to lower Rayleigh numbers and higher wave numbers, indicating a destabilization of the flow, whereas for gas heating $\mu^* > 1$, the opposite trend is true.

The critical Rayleigh number and wave number are plotted as a function of Ra_d for selected values of μ^* and λ in Figures 6 and 7. Observe that, as the variable viscosity parameter μ^* or λ increases, the critical Rayleigh Ra_x^* increases. Also, as Ra_d is increased the critical Rayleigh number Ra_x^* is decreased. Further, the critical wave number k^* is increased as Ra_d and λ are increased and μ^* is decreased. From these figures it can be seen that, the inertia effects reduce the heat transfer rate and destabilize the flow. Finally, we conclude that, the variable viscosity effect enhances the heat transfer rate and destabilizes the flow for liquid heating, while the opposite tend is true for gas heating.

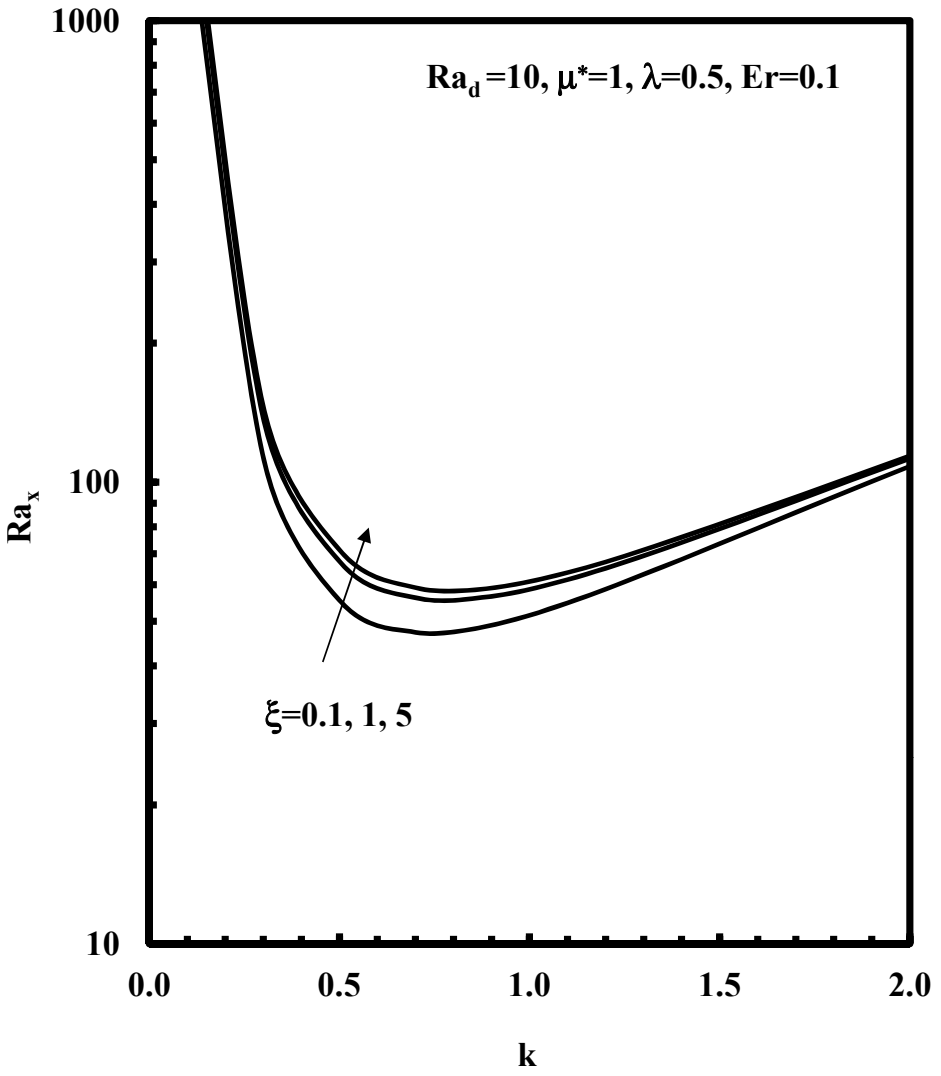

Figure 5 Neutral stability curves for selected values of ξ.

5 Conclusions

The non-Darcy free convection flow on a semi-infinite non-isothermal horizontal plate embedded in a porous medium with variable viscosity is investigated. The effects of variable viscosity characterized by the parameter μ^* on the flow and vortex instability are examined. The governing partial differential equations are transformed to a non similar form by introducing appropriate transformations and are solved numerically using an implicit finite difference scheme. The resulting eigenvalue problem is solved by using a finite difference scheme. The effects of all involved parameters on the local Nusselt number, critical Rayleigh and associated wave number are presented. The results show that, for liquid heating, the variable viscosity effect enhances the heat transfer rate and destabilizes flow; for gas heating, the opposite is true.

Nomenclature

a spanwise wave number

d mean particle diameter or pore diameter

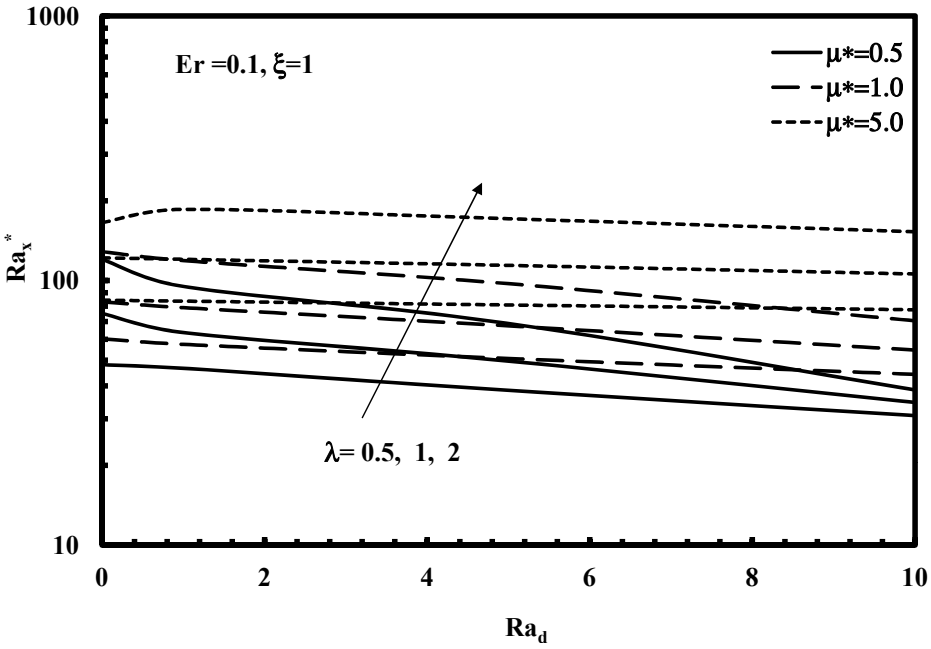

Figure 6 Critical Rayleigh number as a function of Ra_d for selected values of μ^* and λ.

f dimensionless base state stream function
F dimensionless disturbance stream function
g gravitational acceleration
i complex number
k dimensionless wave number
K permeability of porous medium
K^* inertial coefficient in Ergun Equation

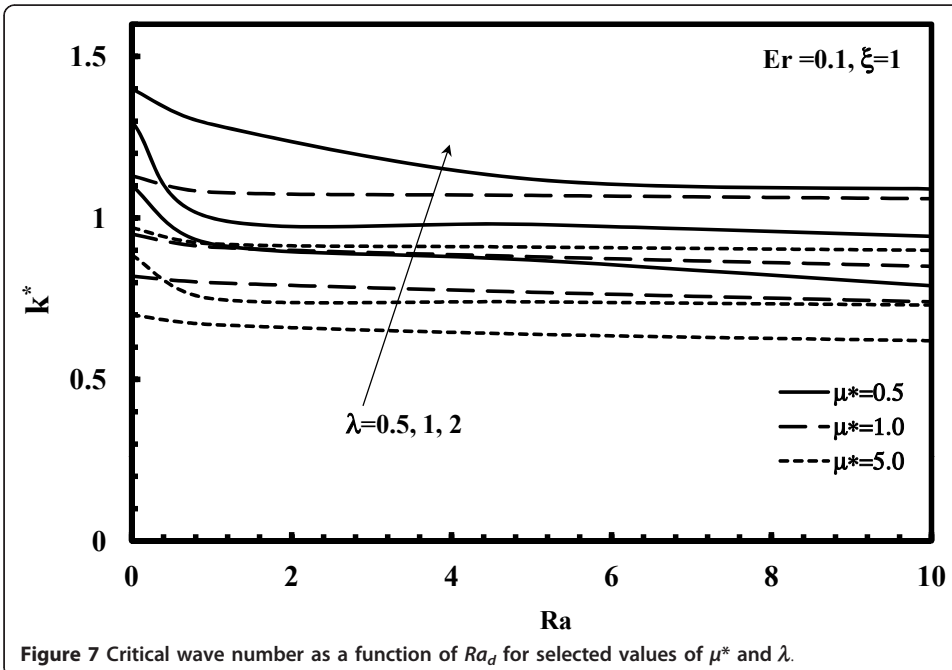

Figure 7 Critical wave number as a function of Ra_d for selected values of μ^* and λ.

Nu_x local Nusselt number

P pressure

Ra_x local Rayleigh number

Ra_d Rayleigh number based on the pore diameter

T fluid temperature

u, v, w volume averaged velocity in the x, y, z directions

x, y, z axial, normal and spanwise coordinates

Greek symbols

α thermal diffusivity

β volumetric coefficient of thermal expansion

η pseudo-similarity variable

θ dimensionless base state temperature

Θ dimensionless disturbance temperature

μ dynamic viscosity of the fluid

ξ non similarity parameter

λ exponent in the wall temperature variation

v kinematic viscosity

μ^* wall to ambient viscosity ratio, $\mu^* = \frac{\mu_w}{\mu_\infty}$

ψ stream function

Subscripts

w conditions at the wall

∞ conditions at the free stream

0 basic undisturbed quantities

1 disturbed quantities

Superscripts

* critical value

' differentiation w.r.t η

Acknowledgements

The authors were grateful to the anonymous reviewers for constructive suggestions and valuable comments, which had improved the quality of the article.

Author details

[1]Department of Mathematics, Faculty of Science, King Abdulaziz University, P.O. Box 80203, Jeddah 21589, Saudi Arabia [2]Department of Mathematics, Faculty of Science for Girls, King Khalid University, Abha, Saudi Arabia [3]Department of Mathematics, University Collage in Makkah, Umm-Alqura University, Makkah, Saudi Arabia [4]Department of Mathematics, Faculty of Science, Al-Azhar University (Assiut Branch), Assiut, Egypt [5]Department of Mathematics, Faculty of Science, Assiut University, Assiut, Egypt

Authors' contributions

All authors participated in the design of the study and performed the numerical simulation. All authors conceived of the study, and participated in its design and coordination. All authors read and approved the final manuscript.

Competing interests

The authors declare that they have no competing interests.

Received: 1 October 2011 Accepted: 27 February 2012 Published: 27 February 2012

References

1. Hsu, CT, Cheng, P, Homsy, GM: Instability of free convection flow over a horizontal impermeable surface in a porous medium. Int J Heat Mass Transfer. **21**, 1221–1228 (1978). doi:10.1016/0017-9310(78)90141-2

2. Jang, JY, Chang, WJ: Vortex instability in buoyancy-induced inclined boundary layer flow in a saturated porous medium. Int J Heat Mass Transfer. **31**, 759–767 (1988). doi:10.1016/0017-9310(88)90133-0
3. Elaiw, AM: Vortex instability of mixed convection boundary layer flow adjacent to a non-isothermal inclined surface in a porous medium with variable permeability. ZAMM Z Angew Math Mech. **88**, 121–128 (2008). doi:10.1002/zamm.200700045
4. Hassanien, IA, Salama, AA, Elaiw, AM: Variable permeability effect on vortex instability of mixed convection flow in a semi-infinite porous medium bounded by a horizontal surface. Appl Math Comput. **146**, 829–847 (2003). doi:10.1016/S0096-3003(02)00635-5
5. Hassanien, IA, Salama, AA, Elaiw, AM: Variable permeability effect on vortex instability of a horizontal natural convection flow in a saturated porous medium with variable wall temperature. ZAMM Z Angew Math Mech. **84**, 39–47 (2004). doi:10.1002/zamm.200410085
6. Elaiw, AM, Ibrahim, FS, Bakr, AA: The influence of variable permeability on vortex instability of a horizontal combined free and mixed convection flow in a saturated porous medium. ZAMM Z Angew Math Mech. **87**, 528–536 (2007). doi:10.1002/zamm.200610334
7. Chang, WJ, Jang, JY: Non-Darcian effects on vortex instability of a horizontal natural convection flow in a saturated porous medium. Int J Heat Mass Transfer. **32**, 529–539 (1989). doi:10.1016/0017-9310(89)90141-5
8. Chang, WJ, Jang, JY: Inertia effects on vortex instability of a horizontal natural convection flow in a saturated porous medium. Int J Heat Mass Transfer. **32**, 541–550 (1989). doi:10.1016/0017-9310(89)90142-7
9. Hassanien, IA, Salama, AA, Moursy, NM: Non-Darcian effects on vortex instability of mixed convection over horizontal plates in porous medium with surface mass flux. Int Commun Heat Mass Transfer. **31**, 231–240 (2004). doi:10.1016/S0735-1933(03)00228-8
10. Hassanien, IA, Salama, AA, Moursy, NM: Inertia effect on vortex instability of horizontal natural convection flow in a saturated porous medium with surface mass flux. Int Comm Heat Mass Transfer. **31**, 741–750 (2004). doi:10.1016/S0735-1933(04)00061-2
11. Lee, DH, Yoon, DY, Choi, CK: The onset of vortex instability in laminar convection flow over an inclined plate embedded in a porous medium. Int J Heat Mass Transfer. **43**, 2895–2908 (2000). doi:10.1016/S0017-9310(99)00337-3
12. Nield, DA, Bejan, A: Convection in Porous Media. Springer Science + Business Media, New York, NY, USA, 3 (2006)
13. Kassoy, DR, Zebib, A: Variable viscosity effects on the onset of convection in porous media. Phys Fluids. **18**, 1649–1651 (1975). doi:10.1063/1.861083
14. Gray, J, Kassoy, DR, Tadjeran, H, Zebib, A: The effect of significant viscosity variation on convective heat transport in water saturated porous media. J Fluid Mech. **117**, 233–249 (1982). doi:10.1017/S0022112082001608
15. Lai, FC, Kulacki, FA: The effect of variable viscosity on convective heat transfer along a vertical surface in a saturated porous medium. Int J Heat Mass Transfer. **33**, 1028–1031 (1990). doi:10.1016/0017-9310(90)90084-8
16. Kumari, M: Effect of variable viscosity on non-Darcy free or mixed convection flow on a horizontal surface in a saturated porous medium. Int Commun Heat Mass Transfer. **28**, 723–732 (2001). doi:10.1016/S0735-1933(01)00276-7
17. Jayanthi, S, Kumari, M: Effect of variable viscosity on non-Darcy free or mixed convection flow on a vertical surface in a fluid saturated porous medium. Mech Res Commun. **33**, 148–156 (2006). doi:10.1016/j.mechrescom.2005.09.001
18. Afify, AA: Effects of variable viscosity on non-Darcy MHD free convection along a non-isothermal vertical surface in a thermally stratified porous medium. Appl Math Model. **31**, 1621–1634 (2007). doi:10.1016/j.apm.2006.05.002
19. Jang, JY, Leu, JS: Variable viscosity effect of on the vortex instability of free convection boundary layer flow over a horizontal surface in porous medium. Int J Heat Mass Transfer. **36**, 1287–1294 (1993). doi:10.1016/S0017-9310(05)80097-3
20. Elaiw, AM, Ibrahim, FS, Bakr, AA, Salama, AA: Effect of variable viscosity on vortex instability of mixed convection boundary layer flow adjacent to a non-isothermal horizontal surface in a porous medium. Arabian J Sci Eng. **36**, 1517–1528 (2011). doi:10.1007/s13369-011-0136-7
21. Ergun, S: Fluid flow through packed columns. Chem Eng Prog. **48**, 89–94 (1952)
22. Sparrow, EM, Quack, H, Boerner, CT: Local nonsimilarity boundary layer solutions. AIAA J. **8**, 1936–1942 (1970). doi:10.2514/3.6029
23. Usmani, RA: Some new finite difference methods for computing eigenvalues of two-point boundary value problems. Comput Math Appl. **9**, 903–909 (1985)
24. IMSL: References Manual. IMSL, Inc., Houston, TX (1990)

doi:10.1186/1687-2770-2012-26
Cite this article as: Elaiw *et al.*: **Effect of variable viscosity on vortex instability of non-Darcy free convection boundary layer flow adjacent to a non-isothermal horizontal surface in a porous medium.** *Boundary Value Problems* 2012 **2012**:26.